Applied Mathematical Modelling 89 (2021) 285–298

Contents lists available at ScienceDirect

Applied Mathematical Modelling

journal homepage: www.elsevier.com/locate/apm

Coupled vibration analysis for equivalent dynamic model of the space antenna truss

Mei Liu[a], Dengqing Cao[a,*], Dongfang Zhu[b]

[a] School of Astronautics, Harbin Institute of Technology, PO Box 137, Harbin 150001, China
[b] Shanghai Aerospace Control Technology Institute, Shanghai 201109, China

ARTICLE INFO

Article history:
Received 24 July 2019
Revised 23 June 2020
Accepted 5 July 2020
Available online 5 August 2020

Keywords:
Antenna truss
Equivalent beam model
Energy equivalence principle
Coupled vibration analysis
Rigid joint
Spatial periodic element

ABSTRACT

A novel equivalent dynamic model is developed for coupled vibration analysis of the space antenna truss to enhance the design capacity of vibration controllers. Based on energy equivalence principle, the space antenna truss with two important features of rigid joints and complicated configuration is equivalent to a spatial anisotropy Timoshenko beam model. According to the kinematic assumptions, strain and kinetic energy expressions of the spatial periodic element can be obtained in accordance with displacement components at its center. Hamilton's principle is carried out to formulate the governing partial differential equations of motion for the equivalent beam model (EBM) which is divided into two sets of PDEs. Each set of PDEs includes three degrees of freedom and describes bending-torsion and bending-extension couplings respectively, due to the asymmetry of the antenna truss. An exact analytical method is developed to solve the two sets of coupled motion equations. The natural characteristics of the EBM are shown to be in excellent agreement with those of the finite element method, which demonstrates that the proposed EBM can provide a satisfactory accuracy for the antenna truss. In addition, since the mode shapes of the EBM are expressed as analytical functions of the spatial coordinate, such an approach may lead the investigations of dynamic property and the design of vibration control law to become convenient for the space antenna truss.

1. Introduction

With progress in aerospace technology, demands for structures are ever-increasing to meet desirable purposes. Due to the limited space in existing rockets, large deployable truss structures are widely used in space applications since they have advantages of light weight, large stiffness to mass ratio and high packaging efficiency [1–3]. Therefore, an approach for investigating the dynamic response of large space antenna trusses has become a crucial and hot topic.

It is urgent to establish a dynamic model effectively and analyze deployable truss structures' dynamic response accurately at control design stage. Applying the finite element method (FEM) is a prevailing approach to calculate the dynamic response for space antenna truss. However, FEM requires a significant amount of computing capacity, and large-order models may be too large to be applied effectively for the design of vibration control systems when structures have features of high freedom, complex configuration and special operation environment [4–6]. To overcome the above drawbacks of FEM, the equivalent

* Corresponding author
E-mail address: dqcao@hit.edu.cn (D. Cao).

https://doi.org/10.1016/j.apm.2020.07.013
0307-904X/

modeling methodology is computationally attractive in modeling structures while providing great convenience for the design of low-order control law [7–10]. Another advantage is that equivalent modeling techniques would generally not capture local modes, reckoning that local models are not of major importance for vibration control design of large structures and only the global dynamic behaviors are required for vibration control applications [5,11,12]. Herein, many researches put efforts to investigate equivalent modeling methods and guarantee their accuracy. In the study of Noor [13], it has been stated that the developments of equivalent modeling and future directions of this research.

In this regard, direct method was applied to find the equivalent stiffness of truss structures [14–16]. This equivalent method leads to huge computational cost for complicated and large trusses since the periodic character of structures is generally not utilized. In another work the transformation matrices were developed to construct the relationship between continuum model and truss structure [17,18]. Lee [19] deduced the transfer matrices by assembling the spectral element matrices for each component within the lattice cell. The equivalent structural properties and vibration characteristics of planar lattice structures were investigated based on spectral element approach. Also, discrete field method [20,21] is carried out to mimic a continuum model for lattice structures. However, with the increase of structural complexity and dimension, this approach will become quite involved. Typically, energy equivalence method and a few different variations have been developed and studied by many researchers. Noor et al. [22] proposed an energy equivalence approach for lattice structure and established continuum models for beamlike and platelike lattice respectively, and this principle were used in several further developments [23,24]. Dow et al. [25] employed a 3-order polynomial to approximate the field displacement, which generates 60 coefficients used for identifying strain-displacement relations. Yildiz et al. [26] follow Dow's work, but applying their method to n-strut cylindrical tensegrity towers considering the geometric nonlinearities. McCallen and Romstad [27,28] founded a simple equivalent continuum model for two-dimensional lattice structures. To accurately approximate the behavior of rigid-joint frames, an additional strain energy term, which is not found in classical Timoshenko beam theory, was introduced in the continuum strain energy function. It should be noted that this simple equivalent continuum model distinguishes from the equivalent micropolar continuum model proposed by Noor and Nemeth [29] when handling truss structures with rigid joints. Besides, a simplification method for spatial X-braced lattice girders with rigid joints was proposed by Wu and Chen [30] based on the static condensation method, which has been demonstrated to be efficient by dynamic analyses. Furthermore, Webster and Velde [31] combined the describing function technique for modeling nonlinearities with an equivalent beam method for modeling trusses and this approach was verified via experiment. But this work focuses on discussing a method of modeling nonlinearities in the truss joints. A homogenization method was performed [32,33] to investigate the equivalent continuum model of planar periodic beam lattice, which involves rigorous mathematical techniques. On the basis of small deformation theory, Zhang et al. [34] developed an equivalent modal method to eliminate air effects for structural dynamic characteristic in ground experiment by making the natural frequencies and vibration modes of the original full-area membrane and the alternative grid membrane identical. Recently, equivalent dynamic models for hoop truss structures [35,36] were put forward to study their dynamic characteristics and accuracies, which successfully employed the energy equivalent principle to generate the stiffness and mass matrices and then solved natural vibration characteristics of equivalent models using FEM. For the rigid-jointed truss structure, Liu et al. [35] tried to construct an equivalent circular ring model based on the classical continuum theory, rather than the micropolar continuum theory. This method avoids a relatively complex derivation proposed by Noor and Nemeth [29], but it is limited to the truss structure with planar repeating element. Furthermore, Liu et al. [37] established an equivalent beam model of a space antenna truss whose spatial repeating element is complex and in initial stress state as compared with [35]. Also, this proposed method in [37] has a simpler derivation procedure compared with the micropolar elasticity theory [29], and thus it is more acceptable for engineers.

In the present study, an equivalent anisotropic Timoshenko beam model of complicated, rigid-jointed and asymmetry space antenna truss with spatial periodic element is proposed based on energy equivalence principle. Then, the governing partial differential equations at six directions for the EBM are worked out using Hamilton's principle. Taking account of the complexity of the antenna truss compared with those reported in the literatures, the difficulties of equivalent modeling grow dramatically. Furthermore, the asymmetry of the antenna truss specifically leads the governing equations of motion of the EBM to two sets of PDEs describing the bending-torsion and bending-extension couplings respectively. To get the natural frequencies and extract the mode shapes of the system, an exact analytical algorithm is developed for bending-torsion and bending-extension coupled dynamic models, which is motivated by the concept proposed in Banerjee and Su [38–40]. In this way, the precision of the natural characteristics of equivalent dynamic model can be better guaranteed.

About the study of coupled beam dynamic problem, efforts were devoted to solve it by many researchers. Beams type structures are widespreadly used in different application fields such as civil, mechanical and aerospace engineering. The dynamic stiffness matrix of airfoil modeled as uniform beam element was derived as an exact method to acquire natural frequencies [41,42], which contains the effect of bending-torsion couplings. Bercin and Tanaka [43] investigated the coupled flexural-torsional vibration of a thin-walled monosymmetric beam as developed by Banerjee [42] and the warping stiffness was taken into account in the formulations. Based on Green's functions, steady-state dynamic response of bending-torsion coupled Timoshenko beam subjected to distributed and concentrated loads was obtained by Han et al. [44]. As is well recognized, interest in functionally graded material has grown enormously. However, the governing differential equations of motion for functionally graded beams are generally coupled due to the variation of the material properties. Su et al. [39] and Banerjee et al. [40] provided an exact method to solve the coupled bending-extensional motion equations for

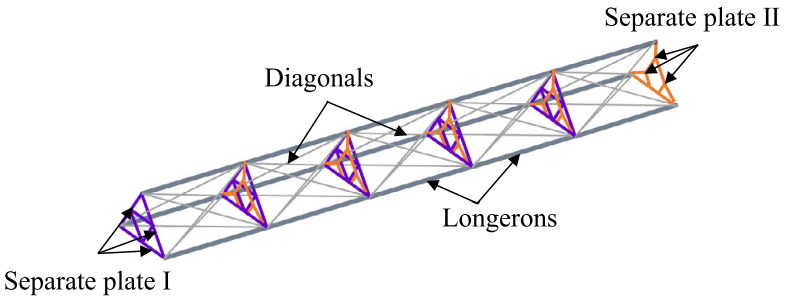

Fig. 1. Space antenna truss in fully expansion.

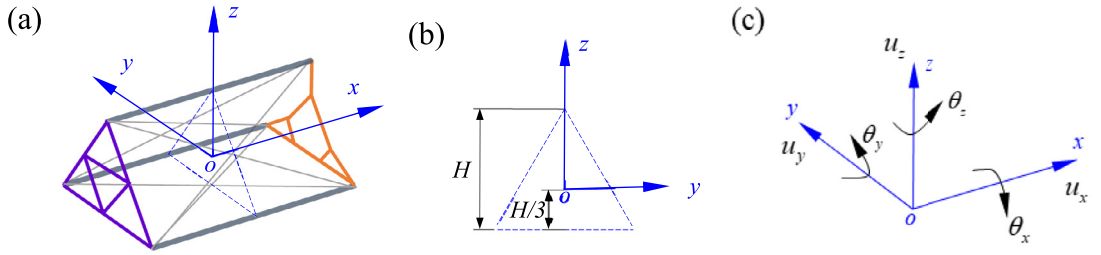

Fig. 2. Schematic view of (a) spatial periodic element, (b) Cartesian coordinate associated with midcross-section and (c) positive direction of displacement components.

functionally graded beams. Similarly, transfer matrix method was employed to analyze the coupled bending-extensional vibration characteristics of a functionally graded Bernoulli-Euler beam in [45].

To the knowledge of the authors, there is no related investigation concerning the exact analytical method for the free vibration analysis of the coupled equivalent beam model of truss structure. In this paper, we focus on solving the vibration characteristics of the equivalent beam model via the analytical approach, for the cantilevered and free-free space antenna trusses. This study is an extension of our previous research [37] in which an equivalent beam model of the truss structure with initial stress was established. It should be noted that the equivalent beam model in Ref. [37] exhibits couplings of six degrees of freedom caused by the initial stress, which leads to a great difficulty to obtain its natural characteristics in analytical solution, and thus the finite element method was employed to solve the natural characteristics. The equivalent beam model of the space antenna truss without initial stress in this study presents bending-torsion and bending-extension couplings characteristics and we develop an exact analytical solution method to solve the two sets of coupled motion equations. In contrast, the analytical solution method has a substantial advantage in the accuracy guarantee. Further, it can provide convenience to the subsequent developments in nonlinear study and controller design of the truss structure. Employing the analytical method developed in Banerjee and Su [38–40], we fill this gap successfully to study the free vibration of the space antenna truss. The bending-torsion and bending-extension coupled governing partial differential equations of motion deduced by the proposed equivalent modeling approach in this study can be solved in closed analytical form giving exact displacement expressions for the natural frequencies and vibration modes of the equivalent anisotropy Timoshenko beam model. This method owns an excellent accuracy because, unlike FEM and other approximate methods, all assumptions made in this method are within the limits of the governing partial differential equations of motion of the structure, without any loss of accuracy [42]. This paper is structured as follows. In Section 2, some kinematic assumptions of the space antenna truss are introduced. Then, based on energy equivalence principle, the equivalent beam model of the antenna truss is proposed and the bending-torsion and bending-extension coupled governing partial differential equations of motion are derived employing Hamilton's principle. Section 3 presents the exact solution method for the two sets of coupled motion equations. The effectiveness and accuracy of the proposed EBM are validated through the comparisons of the results obtained here and those from finite element simulation in Section 4. Finally, conclusions are drawn in Section 5.

2. Equivalent modeling method

A schematic diagram of the space antenna truss studied here has been shown in Fig. 1. The structure has a regular triangular cross section and is constituted of 36 typical spatial periodic elements along the axial direction. The connections of the adjacent periodic elements are rigid-jointed. The spatial periodic element shown in Fig. 2(a) is composed of three longerons, two separate plates, and six diagonals, for which geometrical parameters and material constants are provided in Table 1. The separate plate I and II consists of nine and ten members, and the connections among the adjacent members are rigid-jointed for the separate plates. The longeron and separate plate members are made of tubes and the diagonal

Table 1
Geometrical parameters and material properties of the antenna truss.

Components	Parameters	Values
Longeron	Length L_l (mm)	2740
	Outer diameter D_l (mm)	100
	Thickness t_l (mm)	1
	Inner diameter d_l (mm)	98
	Modulus of elasticity E_l (GPa)	69
	Poisson ratio μ_l	0.33
	Mass density ρ_l (kg/m^3)	2700
Separate plate	Height H (mm)	2771.3
	Outer diameter D_b (mm)	50
	Thickness t_b (mm)	1
	Inner diameter d_b (mm)	48
	Modulus of elasticity E_b (GPa)	370
	Poisson ratio μ_b	0.22
	Mass density ρ_b (kg/m^3)	3960
Diagonal	Length L_d (mm)	4212.8
	Diameter D_d (mm)	6
	Modulus of elasticity E_d (GPa)	88
	Mass density ρ_d (kg/m^3)	1600

members are constructed of bars. Owing to periodic characteristic of this structure, the efforts are only devoted to investigate the kinetic and strain energy expressions of a single periodic element and then use Hamilton's principle to derive governing partial differential equations of motion for this structure. Separating a periodic element from the structure, this paper establishes the Cartesian coordinate system at the center, shown in Fig. 2(b), according to the right-hand rule and the sign convention for displacement and rotation components is illustrated in Fig. 2(c).

2.1. Kinematic assumptions and geometric equations

The displacement and rotation fields of the spatial periodic element presents linear variations in the cross-section and takes the following form:

$$\begin{cases} u_x(x,y,z) = u_x^0(x) - y\theta_z^0(x) + z\theta_y^0(x) \\ u_y(x,y,z) = u_y^0(x) + y\varepsilon_y^0(x) + z(-\theta_x^0(x) + \frac{1}{2}\gamma_{yz}^0(x)) \\ u_z(x,y,z) = u_z^0(x) + y(\theta_x^0(x) + \frac{1}{2}\gamma_{yz}^0(x)) + z\varepsilon_z^0(x) \\ \theta_x = \frac{1}{2}(\frac{\partial u_z}{\partial y} - \frac{\partial u_y}{\partial z}) \\ \theta_y = \frac{1}{2}(\frac{\partial u_x}{\partial z} - \frac{\partial u_z}{\partial x}) \\ \theta_z = \frac{1}{2}(\frac{\partial u_y}{\partial x} - \frac{\partial u_x}{\partial y}) \end{cases} \tag{1}$$

where $u_x^0(x)$, $u_y^0(x)$, $u_z^0(x)$ denote the displacement components at the center of the cross-section $y = 0$, $z = 0$; $\theta_x^0(x)$, $\theta_y^0(x)$, $\theta_z^0(x)$ are the rotation components of the cross section about x, y and z axis, respectively; $\varepsilon_y^0(x)$, $\varepsilon_z^0(x)$ are the extensional strains evaluated at the center of the cross-section in y and z directions, respectively; $\gamma_{yz}^0(x)$ represents the shear strain in plane y-z of the cross-section.

Using the Taylor series expansion method and the classical continuum theory, the displacement field of the spatial periodic element described by the first three formulas in Eq. (1) can be expressed as:

$$\begin{cases} u_x(x,y,z) \approx u_{x0} - y\theta_{z0} + z\theta_{y0} + x\varepsilon_{x0} - xy\kappa_{y0} + xz\kappa_{z0} \\ u_y(x,y,z) \approx u_{y0} + y\varepsilon_{y0} + z(-\theta_{x0} + \frac{1}{2}\gamma_{yz0}) + x(\theta_{z0} + \gamma_{xy0}) - xz\kappa_{x0} + \frac{1}{2}x^2\kappa_{y0} \\ u_z(x,y,z) \approx u_{z0} + y(\theta_{x0} + \frac{1}{2}\gamma_{yz0}) + z\varepsilon_{z0} + x(\gamma_{xz0} - \theta_{y0}) + xy\kappa_{x0} - \frac{1}{2}x^2\kappa_{z0} \end{cases} \tag{2}$$

where u_{x0}, u_{y0}, u_{z0}, θ_{x0}, θ_{y0} and θ_{z0} are displacement and rotation components at the center of the spatial periodic element; ε_{x0}, ε_{y0}, ε_{z0}, γ_{xy0}, γ_{xz0}, γ_{yz0}, κ_{x0}, κ_{y0} and κ_{z0} are strain and curvature measures evaluated corresponding positon. Substituting coordinate of one point into Eq. (2), the corresponding displacements and rotations can be obtained. The strain components of the EBM ε_{x0}, γ_{xy0}, γ_{xz0}, κ_{x0}, κ_{y0}, κ_{z0} can describe the displacements and rotations corresponding to the spatial periodic element on the basis of the geometric equations:

$$\begin{aligned} &\theta_{y0} = -\left.\frac{du_z^0(x)}{dx}\right|_{x=0} + \gamma_{xz0}, \quad \theta_{z0} = \left.\frac{du_y^0(x)}{dx}\right|_{x=0} - \gamma_{xy0}, \quad \varepsilon_{x0} = \left.\frac{du_x^0(x)}{dx}\right|_{x=0}, \\ &\kappa_{x0} = \left.\frac{d\theta_x^0(x)}{dx}\right|_{x=0}, \qquad \kappa_{y0} = \left.\frac{d\theta_z^0(x)}{dx}\right|_{x=0}, \qquad \kappa_{z0} = \left.\frac{d\theta_y^0(x)}{dx}\right|_{x=0}. \end{aligned} \tag{3}$$

It should be noted that the equivalent modeling method in this study is extended from two-dimensional periodic element, proposed by Liu et al. [35], to three-dimensional periodic element. Displacement field at three directions is considered in the displacement and rotation expressions Eq. (2) and the strain-displacement relationships Eq. (3), which broadens the application scope of this equivalent modeling method.

2.2. Strain energy of spatial periodic element

Regarding the longerons and the separate plate members as spatial beam elements, and the diagonals as spatial link elements, the strain energy expression of the periodic element can be defined as:

$$U_e = \sum_{\text{members}} \frac{1}{2} \boldsymbol{w}^{(k)T} \boldsymbol{T}^{(k)T} \boldsymbol{K}^{(k)} \boldsymbol{T}^{(k)} \boldsymbol{w}^{(k)} \tag{4}$$

where U_e refers to strain energy of periodic element; k refers to number of the members; $\boldsymbol{w}_i = \{u_{xi}, u_{yi}, u_{zi}, \theta_{xi}, \theta_{yi}, \theta_{zi}\}^T$ refers to displacement vector of node i; $\boldsymbol{w}^{(k)} = \{\boldsymbol{w}_i^T, \boldsymbol{w}_j^T\}^T$ stands for displacement vector of node i and j of the kth member; $\boldsymbol{K}^{(k)}$ denotes stiffness matrix of the kth member; $\boldsymbol{T}^{(k)}$ denotes coordinate transformation matrix of the kth member.

Then, the Eq. (4) is described by 6 strain and 3 curvature measures, namely:

$$U_e = U_e(\varepsilon_{x0}, \varepsilon_{y0}, \varepsilon_{z0}, \gamma_{xy0}, \gamma_{xz0}, \gamma_{yz0}, \kappa_{x0}, \kappa_{y0}, \kappa_{z0}) \tag{5}$$

The classical beam assumption in which the longitudinal fibers do not compress each other results in the following:

$$\frac{\partial U_e}{\partial \varepsilon_{y0}} = \frac{\partial U_e}{\partial \varepsilon_{z0}} = \frac{\partial U_e}{\partial \gamma_{yz0}} = 0 \tag{6}$$

Therefore, the strain measures ε_{y0}, ε_{z0} and γ_{yz0} are eliminated and the final form of strain energy can be found in terms of the 6 independent strain components ε_{x0}, κ_{y0}, κ_{z0}, κ_{x0}, γ_{xz0} and γ_{xy0} as follows:

$$U_e = \frac{1}{2}(C_{11}\varepsilon_{x0}^2 + C_{22}\kappa_{y0}^2 + C_{33}\kappa_{z0}^2 + C_{44}\kappa_{x0}^2 + C_{55}\gamma_{xz0}^2 + C_{66}\gamma_{xy0}^2 + C_{13}\varepsilon_{x0}\kappa_{z0}) \tag{7}$$

where C_{11}, C_{22}, C_{33}, C_{44}, C_{55}, C_{66} and C_{13} are strain energy coefficients.

As is evident from Eq. (7), the strain energy includes a non-quadratic term which is related to the coupling between the extension term ε_{x0} and the bending term κ_{z0} in the antenna truss, which is caused by the antenna truss structural asymmetry.

2.3. Kinetic energy of spatial periodic element

According to the displacement derivative versus time, the kinetic energy expression of the spatial periodic element is computed as

$$T_e = \sum_{\text{members}} \frac{1}{2} \dot{\boldsymbol{w}}^{(k)T} \boldsymbol{T}^{(k)T} \boldsymbol{M}^{(k)} \boldsymbol{T}^{(k)} \dot{\boldsymbol{w}}^{(k)} \tag{8}$$

where T_e is kinetic energy of spatial periodic element; k and $\boldsymbol{w}^{(k)}$ denote the same intentions as Eq. (4); "•" is derivative versus time; $\boldsymbol{M}^{(k)}$ stands for mass matrix of kth member; $\boldsymbol{T}^{(k)}$ stands for coordinate transformation matrix of kth member.

The strain terms are ignored and the kinetic energy of the spatial periodic element only contains rigid displacement of members. The kinetic energy formula can then be expressed below.

$$\begin{aligned} T_e = \frac{1}{2}(&B_{11}\dot{u}_{x0}^2 + B_{22}\dot{u}_{y0}^2 + B_{33}\dot{u}_{z0}^2 + B_{44}\dot{\theta}_{x0}^2 + B_{55}\dot{\theta}_{y0}^2 + B_{66}\dot{\theta}_{z0}^2 \\ &+ B_{15}\dot{u}_{x0}\dot{\theta}_{y0} + B_{24}\dot{u}_{y0}\dot{\theta}_{x0} + B_{26}\dot{u}_{y0}\dot{\theta}_{z0} + B_{35}\dot{u}_{z0}\dot{\theta}_{y0} + B_{46}\dot{\theta}_{x0}\dot{\theta}_{z0}) \end{aligned} \tag{9}$$

where B_{11}, B_{22}, B_{33}, B_{44}, B_{55}, B_{66}, B_{15}, B_{24}, B_{26}, B_{35} and B_{46} refer to kinetic energy coefficients. Similar to the previous strain energy expression, the kinetic energy also involves five velocity component couplings according to the Eq. (9).

2.4. Governing partial differential equations of motion

Before deducing governing partial differential equations of motion of the equivalent beam model, the strain and kinetic formulas for the EBM are presented using energy equivalence principle. Combining the Timoshenko beam theory and the Saint Venant theory for torsion, the torsion is assumed to be uniform along the axis without axial warping. Based on the energy equivalence principle ignoring the strain derivative, we obtain the strain energy expression of EBM as:

$$U_B = \frac{1}{2}\int_0^{L_t} \left[\overline{EA}\, u_x'^2 + \overline{EI}_z\theta_z'^2 + \overline{EI}_y\theta_y'^2 + \overline{GJ}\theta_x'^2 + \overline{GA}_{xz}(\theta_y + u_z')^2 + \overline{GA}_{xy}(u_y' - \theta_z)^2 + 2\eta_{13}u_x'\theta_y'\right] dx \tag{10}$$

where $\overline{EA}$, $\overline{EI}_z$, $\overline{EI}_y$, $\overline{GJ}$, $\overline{GA}_{xz}$ and $\overline{GA}_{xy}$ stand for extension, bending, torsion and shear rigidities of EBM; η_{13} is coupling coefficient of stiffness. L_t is total length of antenna truss. Superscript "′" stands for derivative with respect to x coordinate. In accordance with Eq. (7), the coefficients of stiffness are

$$\overline{EA} = \frac{C_{11}}{L}, \quad \overline{EI}_z = \frac{C_{22}}{L}, \quad \overline{EI}_y = \frac{C_{33}}{L}, \quad \overline{GJ} = \frac{C_{44}}{L}, \quad \overline{GA}_{xz} = \frac{C_{55}}{L}, \quad \overline{GA}_{xy} = \frac{C_{66}}{L}, \quad \eta_{13} = \frac{C_{13}}{2L} \tag{11}$$

where L represents the length of periodic element.

Similarly, the kinetic energy expression of EBM can be given as

$$T_B = \frac{1}{2}\int_0^{L_t} \left[\overline{\rho A}\,\dot{u}_x^2 + \overline{\rho A}\,\dot{u}_y^2 + \overline{\rho A}\,\dot{u}_z^2 + \bar{J}_x\dot{\theta}_x^2 + \bar{J}_y\dot{\theta}_y^2 + \bar{J}_z\dot{\theta}_z^2 + 2m_{15}\dot{u}_x\dot{\theta}_y + 2m_{24}\dot{u}_y\dot{\theta}_x + 2m_{26}\dot{u}_y\dot{\theta}_z + 2m_{35}\dot{u}_z\dot{\theta}_y + 2m_{46}\dot{\theta}_x\dot{\theta}_z\right] dx \tag{12}$$

where $\overline{\rho A}$ denotes the mass unit length of EBM; $\bar{J}_x$, $\bar{J}_y$, $\bar{J}_z$ denote the rotational inertia unit length of EBM about x, y and z axis, respectively; m_{15}, m_{24}, m_{26}, m_{35} and m_{46} are coupling coefficients of mass. By means of the Eq. (9), the coefficients of mass are computed as

$$\begin{aligned} &\overline{\rho A} = \frac{B_{11}}{L} = \frac{B_{22}}{L} = \frac{B_{33}}{L}, \quad \bar{J}_x = \frac{B_{44}}{L}, \quad \bar{J}_y = \frac{1}{L}\left(B_{55} - \frac{1}{12}\overline{\rho A}L^3\right), \quad \bar{J}_z = \frac{1}{L}\left(B_{66} - \frac{1}{12}\overline{\rho A}L^3\right), \\ &m_{15} = \frac{B_{15}}{2L}, \quad m_{24} = \frac{B_{24}}{2L}, \quad m_{26} = \frac{B_{26}}{2L}, \quad m_{35} = \frac{B_{35}}{2L}, \quad m_{46} = \frac{B_{46}}{2L} \end{aligned} \tag{13}$$

The above derivation process about the equivalent modeling method is brief. And, the details are presented in Ref. [37] for interested readers.

Having the strain and kinetic energy expressions of the EBM, Hamilton's principle is carried out to formulate the governing partial differential equations of motion for the EBM. The six directions of governing equations u_x, u_y, u_z, θ_x, θ_y and θ_z are derived substituting Eqs. (10) and (12) into Hamilton's equation, which can be stated in the form:

$$\int_{t_1}^{t_2} \delta(T_B - U_B)\, dt = 0 \tag{14}$$

According to variation principle and assumed conditions that these variations are zeros at the boundaries, two sets of coupled governing partial differential equations of motion of the EBM can then be obtained. For the bending-torsion coupled vibration of equivalent Timoshenko beam, the equations of motion along the u_y, θ_x and θ_z are eventually derived

$$\begin{cases} \overline{EI}_z\theta_z'' - \overline{GA}_{xy}\theta_z + \overline{GA}_{xy}u_y' - \bar{J}_z\ddot{\theta}_z - m_{26}\ddot{u}_y - m_{46}\ddot{\theta}_x = 0 \\ \overline{GA}_{xy}u_y'' - \overline{GA}_{xy}\theta_z' - \overline{\rho A}\ddot{u}_y - m_{24}\ddot{\theta}_x - m_{26}\ddot{\theta}_z = 0 \\ \overline{GJ}\theta_x'' - \bar{J}_x\ddot{\theta}_x - m_{24}\ddot{u}_y - m_{46}\ddot{\theta}_z = 0 \end{cases} \tag{15}$$

and for the bending-extension coupled vibration of the three other directions u_x, u_z and θ_y, we arrive at

$$\begin{cases} \overline{EI}_y\theta_y'' + \eta_{13}u_x'' - \overline{GA}_{xz}\theta_y - \overline{GA}_{xz}u_z' - \bar{J}_y\ddot{\theta}_y - m_{15}\ddot{u}_x - m_{35}\ddot{u}_z = 0 \\ \overline{GA}_{xz}u_z'' + \overline{GA}_{xz}\theta_y' - \overline{\rho A}\ddot{u}_z - m_{35}\ddot{\theta}_y = 0 \\ \overline{EA}u_x'' + \eta_{13}\theta_y'' - \overline{\rho A}\ddot{u}_x - m_{15}\ddot{\theta}_y = 0 \end{cases} \tag{16}$$

According to Eqs. (15) and (16), the EBM of the antenna truss displays both bending-torsion and bending-extension couplings. Actually, the centroid position of the separate plate II as shown in Fig. 2(a) is not on the x-axis that is the centroid axis of the regular triangular cross section surrounded by the three longerons. Such an eccentric behavior results in the bending-torsion coupling of the system. And, the bending-extension coupling is a result of the eccentric behavior of the system which is caused by the mono-symmetry of the separate plate II. The motivation of present study for this coupled phenomenon arose initially from the equivalent dynamic modeling. For the dynamic characteristic analysis of coupled Timoshenko beam, many researchers have paid attention to the solution for this problem. In the subsequent section, we will perform an exact and elegant analytical method proposed by Banerjee [38] to solve the vibration characteristics for the bending-torsion coupled equivalent beam model. More importantly, to the best knowledge of the authors, there is no related investigation concerning this exact analytical method within the coupled equivalent beam model. The next presented work will fill this gap.

3. Coupled vibration solution method

In this section, the solving process for the coupled bending-torsional governing partial differential equations of motion is presented in detail. It should be mentioned that the Eqs. (15) and (16) are decoupled obviously. Therefore, we choose the Eq. (15) as example to demonstrate its solution and take the same theory to determine the natural frequencies and mode shapes according to the coupled bending-extension Eq. (16).

The natural boundary conditions are obtained in the process as a by-product of Hamiltonian formulation. The expressions for bending moment M, shear force $S$and torsional moment $T$are obtained as

$$M = -\overline{EI}_z\theta_z', \qquad S = -\overline{GA}_{xy}u_y' + \overline{GA}_{xy}\theta_z, \qquad T = -\overline{GJ}\theta_x' \tag{17}$$

Assuming harmonic oscillation, the displacement and rotations can be represented in the following forms:

$$u_y(x,t) = U_y(x)e^{i\omega t}, \qquad \theta_z(x,t) = \Theta_z(x)e^{i\omega t}, \qquad \theta_x(x,t) = \Theta_x(x)e^{i\omega t} \tag{18}$$

where $U_y(x)$, $\Theta_z(x)$ and $\Theta_x(x)$ are amplitudes of u_y, θ_z and θ_x, respectively. ω is the angular or circular frequency.

Introducing the differential operator $D = d/d\xi$ and the non-dimensional length ξ as

$$\xi = x/L_t \tag{19}$$

The differential equations of motion in Eq. (15) are transformed into the following form:

$$\begin{cases} \left(\bar{J}_z\omega^2 - \overline{GA}_{xy}\right)L^2\Theta_z(\xi) + \overline{EI}_z D^2\Theta_z(\xi) + m_{26}\omega^2L^2U_y(\xi) + m_{46}\omega^2L^2\Theta_x(\xi) + \overline{GA}_{xy}LDU_y(\xi) = 0 \\ \overline{GA}_{xy}D^2U_y(\xi) - \overline{GA}_{xy}LD\Theta_z(\xi) + m_{24}\omega^2L^2\Theta_x(\xi) + m_{26}\omega^2L^2\Theta_z(\xi) + \overline{\rho A}\omega^2L^2U_y(\xi) = 0 \\ \overline{GJ}D^2\Theta_x(\xi) + m_{24}\omega^2L^2U_y(\xi) + m_{46}\omega^2L^2\Theta_z(\xi) + \bar{J}_x\omega^2L^2\Theta_x(\xi) = 0 \end{cases} \tag{20}$$

The coefficients of the differential operators D and D^2 are constants in Eq. (20), and the above three equations can be combined into one six order ordinary differential equation, which satisfies each of $U_y(\xi)$, $\Theta_z(\xi)$ and $\Theta_x(\xi)$ so as to give

$$\left(D^6 + aD^4 - bD^2 - c\right)\Lambda = 0 \tag{21}$$

where

$$\Lambda = U_y(\xi),\ \Theta_z(\xi)\ or\ \Theta_x(\xi) \tag{22}$$

and

$$\begin{cases} a = \frac{\left(\overline{\rho A}\cdot\overline{EI}_z + \overline{GA}_{xy}\cdot\bar{J}_z\right)\cdot\overline{GJ} + \overline{EI}_z\cdot\overline{GA}_{xy}\cdot\bar{J}_x}{\overline{EI}_z\cdot\overline{GA}_{xy}\cdot\overline{GJ}}\omega^2L^2 \\ b = -\frac{\left(\left(\bar{J}_x\cdot\bar{J}_z - m_{46}{}^2\right)\cdot\overline{GA}_{xy} + \left(\overline{\rho A}\cdot\bar{J}_z - m_{26}{}^2\right)\cdot\overline{GJ} + \left(\overline{\rho A}\cdot\bar{J}_x - m_{24}{}^2\right)\cdot\overline{EI}_z\right)\cdot\omega^2 - \overline{\rho A}\cdot\overline{GA}_{xy}\cdot\overline{GJ}}{\overline{EI}_z\cdot\overline{GA}_{xy}\cdot\overline{GJ}}\omega^2L^4 \\ c = -\frac{\left(\left(\bar{J}_x\cdot\bar{J}_z - m_{46}{}^2\right)\cdot\overline{\rho A} - \bar{J}_x\cdot m_{26}{}^2 - \bar{J}_z\cdot m_{24}{}^2 + 2\cdot m_{24}\cdot m_{26}\cdot m_{46}\right)\cdot\omega^2 - \left(\overline{\rho A}\cdot\bar{J}_x - m_{24}{}^2\right)\cdot\overline{GA}_{xy}}{\overline{EI}_z\cdot\overline{GA}_{xy}\cdot\overline{GJ}}\omega^4L^6 \end{cases} \tag{23}$$

Assuming the solution of in the form $\Lambda = e^{\lambda\xi}$ the characteristic or auxiliary equation of the differential equation Eq. (21) is then given by

$$\lambda^6 + a\lambda^4 - b\lambda^2 - c = 0 \tag{24}$$

Eq. (24) can be reduced to a cubic equation, as

$$\mu^3 + a\mu^2 - b\mu - c = 0 \tag{25}$$

where

$$\mu = \lambda^2 \tag{26}$$

Employing a technique similar to the one described in [38], the solution Λ in Eq. (21) can be expressed in terms of trigonometric and hyperbolic functions, which are capable of avoiding complex arithmetic and improve computational efficiency. In Ref. [41], the reasonability of the solution forms has been demonstrated in detail. Above all, if the roots of Eq. (25) are α, β and γ, the solution Λ is shown as below

$$\Lambda(\xi) = A_1\cosh\alpha\xi + A_2\sinh\alpha\xi + A_3\cos\beta\xi + A_4\sin\beta\xi + A_5\cos\gamma\xi + A_6\sin\gamma\xi \tag{27}$$

where $A_1 - A_6$ are constants and

$$\begin{cases} \alpha = \left[2(q/3)^{1/2}\cos(\phi/3) - a/3\right]^{1/2} \\ \beta = \left[2(q/3)^{1/2}\cos\{(\pi - \phi)/3\} + a/3\right]^{1/2} \\ \gamma = \left[2(q/3)^{1/2}\cos\{(\pi + \phi)/3\} + a/3\right]^{1/2} \end{cases} \tag{28}$$

with

$$\begin{cases} q = b + a^2/3 \\ \phi = \cos^{-1}\left[\left(27c - 9ab - 2a^3\right)/\left\{2\left(a^2 + 3b\right)^{3/2}\right\}\right] \end{cases} \tag{29}$$

$\Lambda(\xi)$ in Eq. (27) can be used to stand for the bending displacement $U_y(\xi)$, bending rotation $\Theta_z(\xi)$, or torsional rotation $\Theta_x(\xi)$, containing three sets of six constants as follows

$$\begin{cases} U_y(\xi) = P_1\cosh\alpha\xi + P_2\sinh\alpha\xi + P_3\cos\beta\xi + P_4\sin\beta\xi + P_5\cos\gamma\xi + P_6\sin\gamma\xi \\ \Theta_z(\xi) = Q_1\cosh\alpha\xi + Q_2\sinh\alpha\xi + Q_3\cos\beta\xi + Q_4\sin\beta\xi + Q_5\cos\gamma\xi + Q_6\sin\gamma\xi \\ \Theta_x(\xi) = R_1\cosh\alpha\xi + R_2\sinh\alpha\xi + R_3\cos\beta\xi + R_4\sin\beta\xi + R_5\cos\gamma\xi + R_6\sin\gamma\xi \end{cases} \tag{30}$$

where only one set of constants are independent. The choice of relating two sets of the six constants in terms of the third one is arbitrary. $P_1 - P_6$ are chosen to be the base set of constants to be related with the other two set of constants. Substituting Eq. (30) into Eq. (20), the following relationships are derived

$$\begin{aligned} Q_1 &= \frac{k_4+k_5\alpha^2}{k_1+k_2\alpha^2+k_3\alpha^4}P_1 + \frac{k_6\alpha+k_7\alpha^3}{k_1+k_2\alpha^2+k_3\alpha^4}P_2, \quad Q_2 = \frac{k_6\alpha+k_7\alpha^3}{k_1+k_2\alpha^2+k_3\alpha^4}P_1 + \frac{k_4+k_5\alpha^2}{k_1+k_2\alpha^2+k_3\alpha^4}P_2, \\ Q_3 &= \frac{k_4-k_5\beta^2}{k_1-k_2\beta^2+k_3\beta^4}P_3 + \frac{k_6\beta-k_7\beta^3}{k_1-k_2\beta^2+k_3\beta^4}P_4, \quad Q_4 = -\frac{k_6\beta-k_7\beta^3}{k_1-k_2\beta^2+k_3\beta^4}P_3 + \frac{k_4-k_5\beta^2}{k_1-k_2\beta^2+k_3\beta^4}P_4, \\ Q_5 &= \frac{k_4-k_5\gamma^2}{k_1-k_2\gamma^2+k_3\gamma^4}P_5 + \frac{k_6\gamma-k_7\gamma^3}{k_1-k_2\gamma^2+k_3\gamma^4}P_6, \quad Q_6 = -\frac{k_6\gamma-k_7\gamma^3}{k_1-k_2\gamma^2+k_3\gamma^4}P_5 + \frac{k_4-k_5\gamma^2}{k_1-k_2\gamma^2+k_3\gamma^4}P_6 \end{aligned} \tag{31}$$

where

$$\begin{cases} k_1 = \left(\left(-\bar{J}_x\cdot\bar{J}_z + m_{46}{}^2\right)\omega^2 + \overline{GA}_{xy}\cdot\bar{J}_x\right)\omega^2L^4 \\ k_2 = \left(\left(-\overline{EI}_z\cdot\bar{J}_x - \overline{GJ}\cdot\bar{J}_z\right)\omega^2 + \overline{GA}_{xy}\cdot\overline{GJ}\right)L^2 \\ k_3 = -\overline{EI}_z\cdot\overline{GJ} \\ k_4 = \left(\bar{J}_x\cdot m_{26} - m_{24}\cdot m_{46}\right)\omega^4L^4 \\ k_5 = \overline{GJ}\cdot m_{26}\cdot\omega^2L^2 \\ k_6 = \overline{GA}_{xy}\cdot\bar{J}_x\cdot\omega^2L^3 \\ k_7 = \overline{GA}_{xy}\cdot\overline{GJ}\cdot L \end{cases} \tag{32}$$

then

$$\begin{aligned} R_1 &= -\frac{k_8+k_9\alpha^2}{k_1+k_2\alpha^2+k_3\alpha^4}P_1 - \frac{k_{10}\alpha}{k_1+k_2\alpha^2+k_3\alpha^4}P_2, \quad R_2 = -\frac{k_{10}\alpha}{k_1+k_2\alpha^2+k_3\alpha^4}P_1 - \frac{k_8+k_9\alpha^2}{k_1+k_2\alpha^2+k_3\alpha^4}P_2, \\ R_3 &= -\frac{k_8-k_9\beta^2}{k_1-k_2\beta^2+k_3\beta^4}P_3 - \frac{k_{10}\beta}{k_1-k_2\beta^2+k_3\beta^4}P_4, \quad R_4 = \frac{k_{10}\beta}{k_1-k_2\beta^2+k_3\beta^4}P_3 - \frac{k_8-k_9\beta^2}{k_1-k_2\beta^2+k_3\beta^4}P_4, \\ R_5 &= -\frac{k_8-k_9\gamma^2}{k_1-k_2\gamma^2+k_3\gamma^4}P_5 - \frac{k_{10}\gamma}{k_1-k_2\gamma^2+k_3\gamma^4}P_6, \quad R_6 = \frac{k_{10}\gamma}{k_1-k_2\gamma^2+k_3\gamma^4}P_5 - \frac{k_8-k_9\gamma^2}{k_1-k_2\gamma^2+k_3\gamma^4}P_6 \end{aligned} \tag{33}$$

where

$$\begin{cases} k_8 = \left(\left(-\bar{J}_z\cdot m_{24} + m_{26}\cdot m_{46}\right)\omega^2 + \overline{GA}_{xy}\cdot m_{24}\right)\omega^2L^4[3pt] \\ k_9 = -\overline{EI}_z\cdot m_{24}\cdot\omega^2L^2 \\ k_{10} = \overline{GA}_{xy}\cdot m_{46}\cdot\omega^2L^3 \end{cases} \tag{34}$$

The expressions for bending moment $M(\xi)$, shear force $S(\xi)$ and torsional moment $T(\xi)$ can be obtained in terms of the constants $P_1 - P_6$, as

$$\begin{aligned} M(\xi) &= -\frac{\overline{EI}_z}{L_t}\frac{d\Theta_z}{d\xi} \\ &= -(\overline{EI}_z/L_t)\{\alpha(e_{\alpha1}\cosh\alpha\xi + e_{\alpha2}\sinh\alpha\xi)P_1 + \alpha(e_{\alpha2}\cosh\alpha\xi + e_{\alpha1}\sinh\alpha\xi)P_2 \\ &\quad + \beta(-e_{\alpha3}\cos\beta\xi - e_{\alpha4}\sin\beta\xi)P_3 + \beta(e_{\alpha4}\cos\beta\xi - e_{\alpha3}\sin\beta\xi)P_4 + \gamma(-e_{\alpha5}\cos\gamma\xi - e_{\alpha6}\sin\gamma\xi)P_5 \\ &\quad + \gamma(e_{\alpha6}\cos\gamma\xi - e_{\alpha5}\sin\gamma\xi)P_6\} \end{aligned} \tag{35}$$

$$\begin{aligned} S(\xi) &= -\frac{\overline{GA}_{xy}}{L_t}\frac{dU_y}{d\xi} + \overline{GA}_{xy}\Theta_z \\ &= \overline{GA}_{xy}\{(-\alpha/L_t\sinh\alpha\xi + e_{\alpha2}\cosh\alpha\xi + e_{\alpha1}\sinh\alpha\xi)P_1 + (-\alpha/L_t\cosh\alpha\xi + e_{\alpha1}\cosh\alpha\xi + e_{\alpha2}\sinh\alpha\xi)P_2 \\ &\quad + (\beta/L_t\sin\beta\xi + e_{\alpha4}\cos\beta\xi - e_{\alpha3}\sin\beta\xi)P_3 + (-\beta/L_t\cos\beta\xi + e_{\alpha3}\cos\beta\xi + e_{\alpha4}\sin\beta\xi)P_4 \\ &\quad + (\gamma/L_t\sin\gamma\xi + e_{\alpha6}\cos\gamma\xi - e_{\alpha5}\sin\gamma\xi)P_5 + (-\gamma/L_t\cos\gamma\xi + e_{\alpha5}\cos\gamma\xi + e_{\alpha6}\sin\gamma\xi)P_6\} \end{aligned} \tag{36}$$

$$
\begin{aligned}
T(\xi) &= -\frac{\overline{GJ}}{L_t}\frac{d\Theta_x}{d\xi} \\
&= -(\overline{GJ}/L_t)\{\alpha(-g_{\alpha1}\cosh\alpha\xi - g_{\alpha2}\sinh\alpha\xi)P_1 + \alpha(-g_{\alpha2}\cosh\alpha\xi - g_{\alpha1}\sinh\alpha\xi)P_2 \\
&\quad + \beta(g_{\alpha3}\cos\beta\xi + g_{\alpha4}\sin\beta\xi)P_3 + \beta(-g_{\alpha4}\cos\beta\xi + g_{\alpha3}\sin\beta\xi)P_4 + \gamma(g_{\alpha5}\cos\gamma\xi + g_{\alpha6}\sin\gamma\xi)P_5 \\
&\quad + \gamma(-g_{\alpha6}\cos\gamma\xi + g_{\alpha5}\sin\gamma\xi)P_6\}
\end{aligned} \tag{37}
$$

where

$$
\begin{aligned}
e_{\alpha1} &= \frac{k_6\alpha + k_7\alpha^3}{k_1 + k_2\alpha^2 + k_3\alpha^4}, \quad e_{\alpha2} = \frac{k_4 + k_5\alpha^2}{k_1 + k_2\alpha^2 + k_3\alpha^4}, \quad e_{\alpha3} = \frac{k_6\beta - k_7\beta^3}{k_1 - k_2\beta^2 + k_3\beta^4}, \\
e_{\alpha4} &= \frac{k_4 - k_5\beta^2}{k_1 - k_2\beta^2 + k_3\beta^4}, \quad e_{\alpha5} = \frac{k_6\gamma - k_7\gamma^3}{k_1 - k_2\gamma^2 + k_3\gamma^4}, \quad e_{\alpha6} = \frac{k_4 - k_5\gamma^2}{k_1 - k_2\gamma^2 + k_3\gamma^4}
\end{aligned} \tag{38}
$$

and

$$
\begin{aligned}
g_{\alpha1} &= \frac{k_{10}\alpha}{k_1 + k_2\alpha^2 + k_3\alpha^4}, \quad g_{\alpha2} = \frac{k_8 + k_9\alpha^2}{k_1 + k_2\alpha^2 + k_3\alpha^4}, \quad g_{\alpha3} = \frac{k_{10}\beta}{k_1 - k_2\beta^2 + k_3\beta^4}, \\
g_{\alpha4} &= \frac{k_8 - k_9\beta^2}{k_1 - k_2\beta^2 + k_3\beta^4}, \quad g_{\alpha5} = \frac{k_{10}\gamma}{k_1 - k_2\gamma^2 + k_3\gamma^4}, \quad g_{\alpha6} = \frac{k_8 - k_9\gamma^2}{k_1 - k_2\gamma^2 + k_3\gamma^4}
\end{aligned} \tag{39}
$$

By imposing the boundary conditions, the constants $P_1 - P_6$, and consequently $Q_1 - Q_6$ and $R_1 - R_6$, can be calculated, as described in the following part.

3.1. Boundary conditions and frequency equation

The boundary conditions of displacements and forces for the cantilever EBM are as follows. For the clamped end ($\xi = 0$):

$$U_y = 0, \quad \Theta_z = 0, \quad \Theta_x = 0 \tag{40}$$

For the free end ($\xi = 1$):

$$M = 0, \quad S = 0, \quad T = 0 \tag{41}$$

Application of boundary conditions Eq. (40) into Eq. (30) at $\xi = 0$, and Eq. (41) into Eqs. (35)- (37) at $\xi = 1$ will yield equations, which may be written in the matrix form:

$$\boldsymbol{FP} = \boldsymbol{0} \tag{42}$$

where vector $\boldsymbol{P} = [P_1\ P_2\ P_3\ P_4\ P_5\ P_6]^T$ and $\boldsymbol{F}$ is a 6×6non-symmetric matrix, given by

$$
\begin{bmatrix}
1 & 0 & 1 & 0 & 1 & 0 \\
e_{\alpha2} & e_{\alpha1} & e_{\alpha4} & e_{\alpha3} & e_{\alpha6} & e_{\alpha5} \\
-g_{\alpha2} & -g_{\alpha1} & -g_{\alpha4} & -g_{\alpha3} & -g_{\alpha6} & -g_{\alpha5} \\
\alpha\lambda_{e1} & \alpha\lambda_{e2} & \beta\lambda_{e3} & \beta\lambda_{e4} & \gamma\lambda_{e5} & \gamma\lambda_{e6} \\
-\alpha s_{h\alpha} + \lambda_{e2} & -\alpha c_{h\alpha} + \lambda_{e1} & \beta s_{\beta} + \lambda_{e4} & -\beta c_{\beta} - \lambda_{e3} & \gamma s_{\gamma} + \lambda_{e6} & -\gamma c_{\gamma} - \lambda_{e5} \\
\alpha\lambda_{g1} & \alpha\lambda_{g2} & \beta\lambda_{g3} & \beta\lambda_{g4} & \gamma\lambda_{g5} & \gamma\lambda_{g6}
\end{bmatrix} \tag{43}
$$

where

$$
\begin{aligned}
\lambda_{e1} &= e_{\alpha1}\cosh\alpha + e_{\alpha2}\sinh\alpha, \quad \lambda_{e2} = e_{\alpha2}\cosh\alpha + e_{\alpha1}\sinh\alpha, \quad \lambda_{e3} = -e_{\alpha3}\cos\beta - e_{\alpha4}\sin\beta, \\
\lambda_{e4} &= e_{\alpha4}\cos\beta - e_{\alpha3}\sin\beta, \quad \lambda_{e5} = -e_{\alpha5}\cos\gamma - e_{\alpha6}\sin\gamma, \quad \lambda_{e6} = e_{\alpha6}\cos\gamma - e_{\alpha5}\sin\gamma
\end{aligned} \tag{44}
$$

$$
\begin{aligned}
\lambda_{g1} &= -g_{\alpha1}\cosh\alpha - g_{\alpha2}\sinh\alpha, \quad \lambda_{g2} = -g_{\alpha2}\cosh\alpha - g_{\alpha1}\sinh\alpha, \quad \lambda_{g3} = g_{\alpha3}\cos\beta + g_{\alpha4}\sin\beta, \\
\lambda_{g4} &= -g_{\alpha4}\cos\beta + g_{\alpha3}\sin\beta, \quad \lambda_{g5} = g_{\alpha5}\cos\gamma + g_{\alpha6}\sin\gamma, \quad \lambda_{g6} = -g_{\alpha6}\cos\gamma + g_{\alpha5}\sin\gamma
\end{aligned} \tag{45}
$$

$$
\begin{aligned}
c_{h\alpha} &= \cosh\alpha/L_t, \quad c_{\beta} = \cos\beta/L_t, \quad c_{\gamma} = \cos\gamma/L_t \\
s_{h\alpha} &= \sinh\alpha/L_t, \quad s_{\beta} = \sin\beta/L_t, \quad s_{\gamma} = \sin\gamma/L_t
\end{aligned} \tag{46}
$$

The necessary and sufficient condition for nonzero elements in the column vector $\boldsymbol{P}$ of Eq. (42) is that $\det[\boldsymbol{F}(\omega)]$ shall be zero. Thus, non-trivial solutions are calculated by imposing

$$\det[\boldsymbol{F}(\omega)] = 0 \tag{47}$$

Eq. (47) is the frequency equation, which can be numerically solved to give the natural frequencies values of ω by successively tracking the changes of its sign.

Table 2
Comparisons of natural frequencies for bending-torsion coupled vibration for the cantilevered truss.

Mode order	Finite element simulation (Hz)	Equivalent beam model (Hz)	Error (%)
1	0.2081^{b}	0.2101^{b}	0.9633
3	1.2360^{b}	1.2414^{b}	0.4376
5	1.4010^{t}	1.3846^{t}	−1.1672
6	3.2122^{b}	3.2143^{b}	0.0652
8	4.1991^{t}	4.1539^{t}	−1.0754
9	5.7402^{b}	5.7245^{b}	−0.2738
11	6.9866^{t}	6.9245^{t}	−0.8887
13	8.5976^{b}	8.5594^{b}	−0.4449

[a] The superscripts *b, t and e* represent dominant bending mode, torsional mode, extensional mode, respectively.
[b] The meaning of superscripts in the following figures and tables is same as above.

Table 3
Comparisons of natural frequencies for bending-extension coupled vibration for the cantilevered truss.

Mode order	Finite element simulation (Hz)	Equivalent beam model (Hz)	Error (%)
2	0.2081^{b}	0.2101^{b}	0.9536
4	1.2365^{b}	1.2420^{b}	0.4485
7	3.2134^{b}	3.2162^{b}	0.0872
10	5.7436^{b}	5.7302^{b}	−0.2330
12	7.1264^{e}	7.2263^{e}	1.4014
14	8.6058^{b}	8.5734^{b}	−0.3770

Table 4
Comparisons of natural frequencies for bending-torsion coupled vibration for the free-free truss.

Mode order	Finite element simulation (Hz)	Equivalent beam model (Hz)	Error (%)
1	1.2965^{b}	1.3049^{b}	0.6463
3	2.7954^{t}	2.7677^{t}	−0.9908
4	3.3555^{b}	3.3663^{b}	0.3205
6	5.5813^{t}	5.5345^{t}	−0.8382
8	6.0482^{b}	6.0509^{b}	0.0443
9	8.3517^{t}	8.3026^{t}	−0.5879
11	9.0753^{b}	9.0666^{b}	−0.0954
12	11.0999^{t}	11.0741^{t}	−0.2328
13	12.2432^{b}	12.2348^{b}	−0.0685

3.2. Mode shapes

The modal vector $\boldsymbol{P}$ can be acquired once the natural frequencies ω are obtained by Eq. (47). To compute the mode shape coefficient relations of $P_1 - P_6$, constants $P_2 - P_6$ will be expressed in terms of P_1 which is chosen as a base constant. Hence, the Eq. (42) can be expressed as the following reduced order formula

$$\begin{bmatrix} P_2 \\ P_3 \\ P_4 \\ P_5 \\ P_6 \end{bmatrix} = \begin{bmatrix} 0 & 1 & 0 & 1 & 0 \\ e_{\alpha 1} & e_{\alpha 4} & e_{\alpha 3} & e_{\alpha 6} & e_{\alpha 5} \\ -g_{\alpha 1} & -g_{\alpha 4} & -g_{\alpha 3} & -g_{\alpha 6} & -g_{\alpha 5} \\ \alpha\lambda_{e2} & \beta\lambda_{e3} & \beta\lambda_{e4} & \gamma\lambda_{e5} & \gamma\lambda_{e6} \\ -\alpha c_{h\alpha} + \lambda_{e1} & \beta s_{\beta} + \lambda_{e4} & -\beta c_{\beta} - \lambda_{e3} & \gamma s_{\gamma} + \lambda_{e6} & -\gamma c_{\gamma} - \lambda_{e5} \end{bmatrix}^{-1} \begin{bmatrix} -1 \\ -e_{\alpha 2} \\ g_{\alpha 2} \\ -\alpha\lambda_{e1} \\ \alpha s_{h\alpha} - \lambda_{e2} \end{bmatrix} P_1 \tag{48}$$

The other two modal vectors $\boldsymbol{Q}$ and $\boldsymbol{R}$ can be determined by the Eq. (31) and Eq. (33), respectively.

4. Results and discussions

In the presented approach, an EBM is found for the antenna truss and, subsequently, the coupled governing partial differential equations of motion are derived and solved by an exact analytical method. As already stated in the Section 2, the dynamic characteristics for the antenna truss are analyzed by utilizing ANSYS software, which is adopted to demonstrate the efficiency and accuracy of the proposed EBM. For the cantilevered truss and free-free truss, comparisons of the natural frequencies for the EBM and the full-scale FEM model are illustrated in Table 2–5, respectively. It is evident that the combination of the equivalent modeling approach and this solution method for coupled vibration equations can achieve excellent accuracy for natural frequencies according to the error analysis. The highest errors of first 14 orders natural frequencies

Table 5
Comparisons of natural frequencies for bending-extension coupled vibration for the free-free truss.

Mode order	Finite element simulation (Hz)	Equivalent beam model (Hz)	Error (%)
2	1.2967[b]	1.3050[b]	0.6382
5	3.3558[b]	3.3664[b]	0.3172
7	6.0475[b]	6.0528[b]	0.0875
10	9.0747[b]	9.0725[b]	−0.0246
14	12.2447[b]	12.2515[b]	0.0555

for cantilevered and free-free structures are −1.1672%, −0.9908%, for the bending-torsion coupled vibration, and 1.4014%, 0.6382%, for bending-extension coupled vibration, which indicates that the proposed EBM can provide a satisfactory accuracy by comparing with the results of finite element simulation in the analysis of natural frequencies.

It is also interesting to investigate the mode shapes of the antenna truss using full-scale FEM. The bending-torsion coupled mode shapes are shown in Fig. 3, for the cantilevered truss. Obviously, bending-torsion coupled mode shapes are found in 1, 3, 5, 6, 8, 9, 11, 13 orders, which is caused by asymmetry of the cross section and is in contrast to the simple triangular truss without coupled effect. Besides, the numerical results prove that the effect of coupling terms is weak in the lower mode shapes. However, this effect will strengthen gradually with the increase of order.

The bending-extension coupling is a result of the eccentric behavior of the system which is caused by the mono-symmetry of the separate plate II. To study the coupled effect of the bending-extension vibration of the antenna truss, the 12th mode of the cantilevered truss is discussed by using ANSYS software. As can be observed from the Fig. 4, the dominant mode in 12th mode is axial vibration. Moreover, there exists bending vibration shown in the enlarge figure although the effect of the coupling is weak. From the analysis of the 12th mode selected, it can be demonstrated that the axial and bending vibrations are coupled for the antenna truss and there exist interaction between the extension and bending.

Moreover, to fully verify the correctness of the proposed EBM and the solution method for the coupled vibration equations, the bending-torsion coupled mode shapes of the EBM are also performed for the purpose of comparison based on maximum displacement normalized method. These results are shown in Fig. 5. The normalization parameters of displacement components α_y and α_x are defined as below.

$$\begin{cases} \alpha_y = \dfrac{u_y}{\max\{u_{y,\max}, R\theta_{x,\max}\}} \\ \alpha_x = \dfrac{R\theta_x}{\max\{u_{y,\max}, R\theta_{x,\max}\}} \end{cases} \tag{49}$$

where u_y, θ_x denote the displacement components in the Y-direction and torsion rotation around the X-axis at joint positions of antenna truss, respectively; $u_{y,\max}, \theta_{x,\max}$ denote the maximum values of u_y, and θ_x, respectively. Note that the θ_x rotation component of the mode shapes is multiplied by the distance R related to height of cross section in order to compare θ_x directly with the u_y displacement component and R is given as

$$R = \frac{2}{3}H \tag{50}$$

where H is the height of cross-section presented in Fig. 2(b).

As can be observed from the Fig. 5, the mode shapes from the EBM are in good agreement with the FEM results. Therefore, the above validations confirm that the proposed EBM are reliable, effective and highly precise, which can provide great convenience for the design of low-order control law. In addition, the EBM is much more computationally efficient. Simultaneously, it is reasonable to extend the exact analytical solution method to analyze the natural characteristics of the coupled equivalent beam model for the truss structure and this solution approach can offer the promise of optimization studies for the system.

5. Concluding remarks

Equivalent modeling method has significant advantages for the design of vibration controller of large space deployable structures. Furthermore, the exact analytical solution approach for coupled equivalent beam model can offer the promise of straightforward optimization for structures. In consideration of these demands, an extended equivalent dynamic beam model has been proposed for the space antenna truss in this study. Based on energy equivalence principle, the governing partial differential equations of motion for the antenna truss are derived employing Hamilton's principle. In particular, governing equations of motion of the equivalent beam model consist of two sets of PDEs describing the bending-torsion and bending-extension couplings respectively, which results from the asymmetry of the space antenna truss and in contrast to simple triangular truss without coupled effect. An exact analytical approach has been developed to deal with the coupled vibrations of equivalent beam model, and the natural frequencies and mode shapes of the system solved in closed analytical form, which can offer better guarantee on the accuracy of the equivalent beam model.

Numerical contrastive analyses include natural frequencies and modes shapes, for cantilever and free-free equivalent beam model. Results indicate that the equivalent beam model has satisfactory accuracy for analyzing the dynamic characteristics of the antenna truss compared with a standard FEM of the structure for the purpose of validation. Meanwhile,

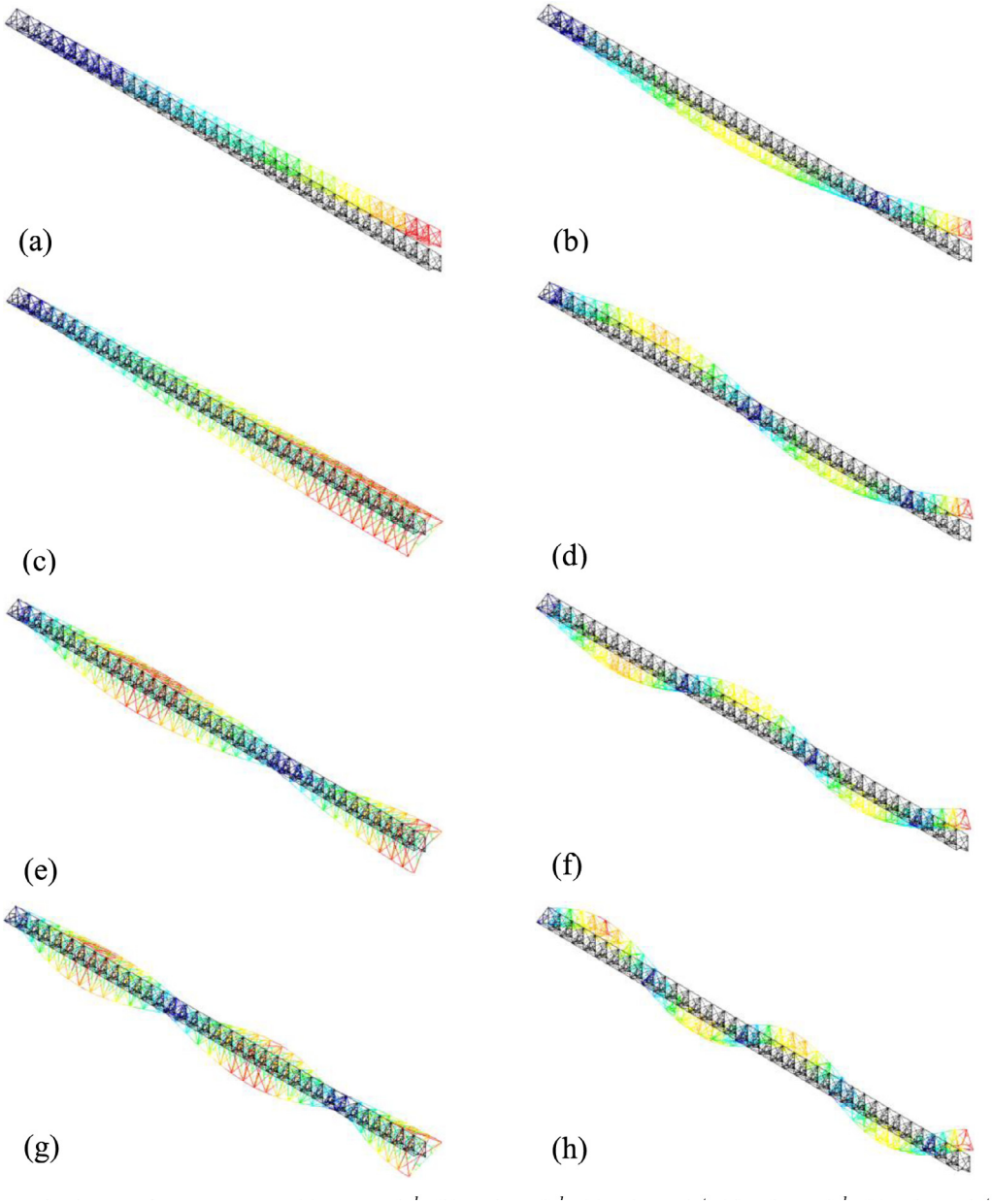

Fig. 3. Mode shapes of antenna truss: (a) 1st mode[b], (b) 3rd mode[b], (c) 5th mode[t], (d) 6th mode[b], (e) 8th mode[t], (f) 9th mode[b], (g) 11th mode[t] and (h) 13th mode[b].

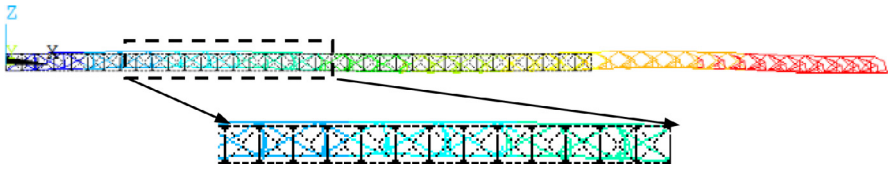

Fig. 4. The 12th mode[e] of the cantilevered truss. (For interpretation of the references to colour in this figure legend, the reader is referred to the web version of this article.)

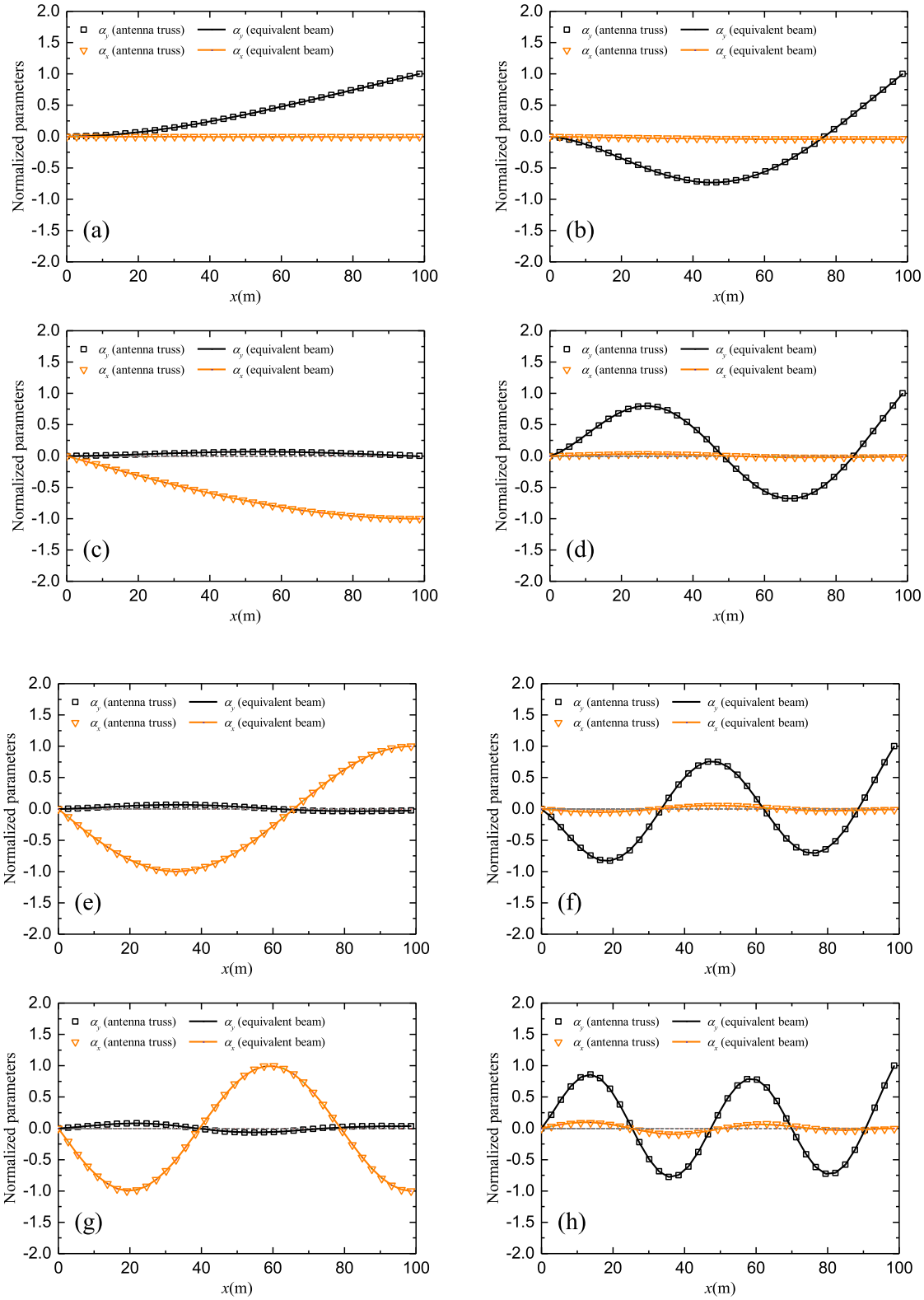

Fig. 5. Comparisons of modes for antenna truss and EBM: (a) 1st mode^b, (b) 3rd mode^b, (c) 5th mode^t, (d) 6th mode^b, (e) 8th mode^t, (f) 9th mode^b, (g) 11th mode^t and (h) 13th mode^b.

the exact analytical solution method for the two sets of coupled partial differential equations turns out to be correct and provides sufficient precision and it has been extended successfully to the research of equivalent dynamic modeling of the antenna truss. This equivalent modeling approach and the exact analytical solution method are useful and possess significant guidance for future designs of low-order control law and optimization problems of large space structure.

Acknowledgements

This research was supported by the National Natural Science Foundation of China (Grant No. 11732005); the Civil Aerospace Project (Grant No. D020213); and the Natural Science Foundation of Shanghai City, PR China (Grant No. 16ZR1415700).

References

[1] M.F. Card, W.J. Boyer, Large space structures-fantasies and facts, in: 21st Structures, Structural Dynamics, and Materials Conference, AIAA Journal, New York, 1980, pp. 101–114. Part 1.
[2] C.H.M. Jenkins, Gossamer spacecraft: membrane and inflatable structures technology for space applications, American Institute of Aeronautics and Astronautics (2001) 191.
[3] G. Kiper, E. Soylemez, in: Deployable Space Structures, IEEE, 2009, pp. 131–138.
[4] S.E. Lamberson, T.Y. Yang, Continuum plate finite elements for vibration analysis and feedback control of space lattice structures, Comput Struct 20 (1–3) (1985) 583–592.
[5] A. Salehian, T.M. Seigler, D.J. Inman, Control of the continuum model of a large flexible space structure, in: Proceedings of the ASME International Mechanical Engineering Congress and Exposition, Chicago, 2006.
[6] Z. Xing, G. Zheng, Deploying process modeling and attitude control of a satellite with a large deployable antenna, Chinese Journal of Aeronautics 27 (2) (2014) 299–312.
[7] R. Padhi, S.F. Ali, An account of chronological developments in control of distributed parameter systems, Annu Rev Control 33 (2009) 59–68.
[8] S. Gonella, M. Ruzzene, Homogenization of vibrating periodic lattice structures, Appl Math Model 32 (2008) 459–482.
[9] B. Yang, C.A. Tan, Transfer functions of one-dimensional distributed parameter systems, ASME Journal Applied Mechanics 59 (1992) 1009–1014.
[10] W.H. Bennett, H.G. Kwatny, Continuum modeling of flexible structures with application to vibration control, AIAA Journal 27 (9) (1989) 1264–1273.
[11] C.T. Sun, S.W. Liebbe, A global-local approach to solving vibration of large truss structures, in: Proceedings of the ASCE/AHS 27th Structures, Structural Dynamics, and Materials Conference, 1986.
[12] C.T. Sun, S.W. Liebbe, Global-local approach to solving vibration of large truss structures, AIAA Journal 28 (2) (1990) 303–308.
[13] A.K. Noor, Continuum modeling for repetitive lattice structures, Appl Mech Rev 41 (7) (1988) 285–296.
[14] W.S. Kenner, N.F. Knight, Soft lattice truss static polynomial response using energy methods, AIAA Journal 36 (6) (1998) 1100–1104.
[15] M.S. Lake, E.C. Klang, Generation and comparison of globally isotropic space-filling truss structures, AIAA Journal 30 (5) (1992) 1416–1424.
[16] C. Gantes, J.J. Connor, R.D. Logcher, Equivalent continuum model for deployable flat lattice structures, Journal of Aerospace Engineering, ASCE 7 (1) (1994) 72–91.
[17] A.H. Nayfeh, M.S. Hefzy, Continuum modeling of the mechanical and thermal behavior of discrete large structures, AIAA Journal 19 (6) (1981) 766–773.
[18] J.O. Dow, Z.W. Su, C.C. Feng, C. Bodley, Equivalent continuum representation of structures composed of repeated elements, AIAA Journal 23 (10) (1985) 1564–1569.
[19] U. Lee, Equivalent continuum representation of lattice beams: spectral element approach, Engineering Structures 20 (7) (1998) 587–592.
[20] J.D. Renton, The beam-like behavior of space trusses, AIAA Journal 22 (2) (1984) 273–280.
[21] H. Tollenaere, D. Caillerie, Continuous modeling of lattice structures by homogenization, Advances in Engineering Software 29 (7–9) (1998) 699–705.
[22] A.K. Noor, M.S. Anderson, W.H. Greene, Continuum models for beam- and platelike lattice structures, AIAA Journal 16 (12) (1978) 1219–1228.
[23] A. Salehian, D.J. Inman, A reduced order micro-polar model of a space antenna with torsional joints, 49th AIAA/ASME/ASCE/AHS/ASC Structures, Structural Dynamics, and Materials Conference, 2008.
[24] A. Salehian, M. Ibrahim, T.M. Seigler, Damping in periodic structures: a continuum modeling approach, AIAA Journal 52 (3) (2014) 569–590.
[25] J.O. Dow, S.A. Huyer, Continuum models of space station structures, J Aerosp Eng 2 (4) (1989) 220–238.
[26] K. Yildiz, G.A. Lesieutre, Effective stiffness properties of n-strut cylindrical tensegrity towers, AIAA Journal 57 (5) (2019) 2185–2194.
[27] D.B. McCallen, K.M. Romstad, A continuum model for the nonlinear analysis of beam-like lattice structures, Comput Struct 29 (2) (1988) 177–197.
[28] D.B. McCallen, K.M. Romstad, A continuum model for lattice structures with geometric and material nonlinearities, Comput Struct 37 (5) (1990) 795–822.
[29] A.K. Noor, M.P. Nemeth, Micropolar beam models for lattice grids with rigid joints, Comput Methods Appl Mech Eng 21 (1980) 249–263.
[30] J.S. Wu, J.M. Chen, Dynamic analysis of spatial beam-like lattice girders, Comput Struct 53 (4) (1994) 961–981.
[31] M. Webster, W.V. Velde, Modeling beam-like space trusses with nonlinear joints, AIAA-91-1225-CP (1991) 2745–2754.
[32] F. Dos Reis, J.F. Ganghoffer, Construction of micropolar continua from the asymptotic homogenization of beam lattices, Computers and Structures 112–113 (2012) 354–363.
[33] F. Penta, L. Esposito, G.P. Pucillo, V. Rosiello, A. Gesualdo, On the homogenization of periodic beam-like structures, Procedia Structural Integrity 8 (2018) 399–409.
[34] Y. Zhang, W. Chen, C. Xie, F. Peng, Modal equivalent method of full-area membrane and grid membrane, Aerospace Systems 1 (2018) 129–137.
[35] F. Liu, D. Jin, H. Wen, Equivalent dynamic model for hoop truss structure composed of planar repeating elements, AIAA Journal 55 (3) (2017) 1058–1063.
[36] H. Guo, C. Shi, M. Li, Z. Deng, R. Liu, Design and dynamic equivalent modeling of double-layer hoop deployable antenna, International Journal of Aerospace Engineering 2018 (2018) 1–15.
[37] M. Liu, D. Cao, D. Zhu, Equivalent dynamic model of the space antenna truss with initial stress, AIAA Journal 58 (4) (2020) 1851–1863.
[38] J.R. Banerjee, Explicit modal analysis of an axially loaded Timoshenko beam with bending–torsion coupling, J Appl Mech 67 (2000) 307–313.
[39] H. Su, J.R. Banerjee, Development of dynamic stiffness method for free vibration of functionally graded Timoshenko beams, Computers and Structures 147 (2015) 107–116.
[40] J.R. Banerjee, A. Ananthapuvirajah, Free vibration of functionally graded beams and frameworks using the dynamic stiffness method, J Sound Vib 422 (2018) 34–47.
[41] J.R. Banerjee, Coupled bending–torsional dynamic stiffness matrix for beam elements, Int J Numer Methods Eng 28 (1989) 1283–1298.
[42] J.R. Banerjee, F.W. Williams, Coupled bending-torsional dynamic stiffness matrix of an axially loaded Timoshenko beam element, Int J Solids Struct 31 (6) (1994) 749–762.
[43] A.N. Bercin, M. Tanaka, Coupled flexural-torsional vibrations of Timoshenko beams, J Sound Vib 207 (1) (1997) 47–59.
[44] H. Han, D. Cao, L. Liu, Green's functions for forced vibration analysis of bending-torsion coupled Timoshenko beam, Appl Math Model 45 (2017) 621–635.
[45] J.W. Lee, J.Y. Lee, Free vibration analysis of functionally graded Bernoulli-Euler beams using an exact transfer matrix expression, International Journal of Mechanical Sciences 122 (2017) 1–17.